

Degenerate Optical Cavities. II: Effect of Misalignments

A. Arnaud

A simple expression is given for the response of degenerate cavities suffering from arbitrary misalignments, and numerical results are presented. The method of resonance excitation is carried out analytically with the help of a complex ray representation of gaussian beams. It is first shown that the modulus and phase of such complex rays can be identified with, respectively, the beam radius and the phase of the on-axis field. This identification simplifies the calculation of the coupling factor between two gaussian beams, which is needed in deriving the expression for the response. For the case of conventional cavities, the results are in exact agreement with results derived from the Laguerre-Gauss or Hermite-Gauss mode theory. The case of degenerate cavities with large and possibly nonorthogonal misalignments, of interest in various nonresonant multipath systems, is also discussed.

I. Introduction

The properties and applications of degenerate optical cavities were discussed in a previous paper.¹ An optical cavity is degenerate when all of the rays retrace their path after a round trip. Such cavities provide frequency filtering without introducing spatial filtering; this is an important feature, in particular, in scanning interferometers. These cavities require, however, a very accurate alignment of their optical elements, in contrast with the case of conventional nondegenerate cavities. A useful consequence is that a degenerate cavity which incorporates a diffraction grating can be made to resonate only in the neighborhood of a selected frequency. The purpose of this paper is to calculate the degradation of the response which results from an arbitrary misalignment and to discuss the influence of the input beam radius and cavity finesse.

The case of large misalignments is also of interest in nonresonant multipath systems such as those used in optical delay lines² and high gain quantum amplifiers³; beam axis patterns more favorable than the Lissajou pattern obtained with conventional cavities can be generated. A degenerate cavity incorporating a time-varying element, such as a rotating mirror, may also be useful for displaying short optical pulses.

A method, called resonance excitation, has been used by Fox and Li⁴ to obtain the mode pattern in optical cavities with the help of a computer. It consists of adding the fields of the successive paths of an incident

beam, reflected back and forth inside the cavity. In this paper, this procedure is carried out analytically, considering an incident beam in the fundamental gaussian mode and neglecting the chopping of the beams at the edges of the optical elements. The total power flowing in the cavity is calculated by integration. This procedure is applicable to any type of cavity, but it is particularly simple in the case in which the cavity is degenerate. The general case of mode degenerate cavities (which includes such cavities as the plane parallel Fabry-Perot) is first considered, and the results are then applied to the special case of degenerate cavities.

Let us now discuss the details of the method. In Secs. II and III, new results relative to the propagation of fundamental gaussian beams are derived. Kogelnik⁵ has shown that the quantity $X(z)$, defined by $q = X/(dX/dz)$, where q is the complex wavefront curvature radius, formally obeys the paraxial ray differential equation, as the beam propagates in a lenslike medium. We attach a physical significance to X and show that its modulus and phase can be identified with, respectively, the beam radius and the phase of the on-axis field.

This representation of fundamental gaussian beams by complex rays is useful in calculating the coupling between two such beams (Sec. IV) and, in particular, the coupling between an input beam and the same beam transformed after r round trips in the cavity. In Sec. V, the response of a cavity is expressed as a function of this coupling factor, and the response of degenerate cavities is considered in detail in Sec. VI. The results obtained for the case of conventional cavities are compared with those derived from the Laguerre-Gauss or Hermite-Gauss mode theory⁶⁻⁸ in the Appendix. The calculations are restricted to nonaberrated orthogonal^{9,10} cavities.

The author is with the Bell Telephone Laboratories, Inc., Crawford Hill Laboratory, Holmdel, New Jersey 07733.

Received 30 January 1969.

II. Propagation of Optical Beams in Misaligned Lenslike Media

Within the first-order optics approximation, the refractive index of a lenslike medium can be written

$$N(x,y,z) = n + \frac{n_x}{n}x + \frac{n_y}{n}y + \frac{n_{xx}}{n}x^2 + \frac{n_{yy}}{n}y^2 + \frac{n_{xy}}{n}xy, \quad (1)$$

in a xyz rectangular coordinate system. n , n_x , n_y , n_{xx} , n_{yy} , and n_{xy} are assumed to be slowly varying complex functions of z , and the terms following n to be small compared with n . Limiting the expansion of N^2 to the first order terms, the wave equation is, from Eq. (1)

$$\frac{\partial^2 E}{\partial x^2} + \frac{\partial^2 E}{\partial y^2} + \frac{\partial^2 E}{\partial z^2} + k^2(n^2 + 2n_x x + 2n_y y + 2n_{xx}x^2 + 2n_{yy}y^2 + 2n_{xy}xy)E = 0, \quad (2)$$

where E is a transverse component of the electric field, and $k = 2\pi/\lambda$ is the free space propagation constant.

If we introduce in Eq. (2) new variables Ψ' and z' , defined by

$$\Psi' = n^{1/2}\Psi, \quad (3a)$$

$$\Psi = E \exp\left(jk \int_0^z n dz\right), \quad (3b)$$

$$z' = \int_0^z dz/n, \quad (3c)$$

and neglect $\partial^2 \Psi / \partial z^2$ because of the slow variation of Ψ with z , we find that Ψ' is solution of

$$\frac{\partial^2 \Psi'}{\partial x^2} + \frac{\partial^2 \Psi'}{\partial y^2} - 2jk \frac{\partial \Psi'}{\partial z'} + 2k^2(n_x x + n_y y + n_{xx}x^2 + n_{yy}y^2 + n_{xy}xy)\Psi' = 0. \quad (4)$$

Equation (4) is a straightforward generalization of the wave equation given in Ref. 5, and is consistent with the scalar Fresnel's diffraction theory. n is henceforth assumed to be unity, without loss of generality, since n does not appear explicitly in Eq. (4). The imaginary part of n must be small compared with its real part, however, for z' to be real valued, and to be interpreted as an axial coordinate. Then, from Eqs. (3a) and (3c) we have $z' \equiv z$ and $\Psi' \equiv \Psi$.

Let us now consider a solution ψ of Eq. (4) with no misalignment terms ($n_x = n_y = 0$), and solutions \bar{x} , \bar{y} of the differential equations:

$$\ddot{\bar{x}} = n_x + 2n_{xx}\bar{x} + n_{xy}\bar{y}, \quad (5a)$$

$$\ddot{\bar{y}} = n_y + 2n_{yy}\bar{y} + n_{xy}\bar{x}, \quad (5b)$$

where the upper dots indicate differentiations with respect to z . By substitution in Eq. (4), we find that

$$\psi(x,y,z) = \psi(x - \bar{x}, y - \bar{y}, z) \times \exp\left[-jk\left(x\dot{\bar{x}} + y\dot{\bar{y}} - \frac{\bar{x}\dot{\bar{x}}}{2} - \frac{\bar{y}\dot{\bar{y}}}{2} + \frac{1}{2} \int_{0_z}^z n_x \bar{x} dz + \frac{1}{2} \int_{0_y}^z n_y \bar{y} dz\right)\right], \quad (6)$$

where 0_x and 0_y are, for the time being, arbitrary points along the z axis, is a solution of the general Eq. (4).

The phase term introduced in Eq. (6) is easily interpreted when n_x , n_y , n_{xx} , n_{yy} , and n_{xy} are real (i.e., when there is no transverse variation of the loss, or the gain). In that case, Eqs. (5a) and (5b) admit real solutions* which represent paraxial rays,¹⁰ and the transformation from $\psi(x,y,z)$ to $\Psi(x,y,z)$ corresponds to a change in beam axis. Let us show that, at $x = \bar{x}$, $y = \bar{y}$, the phase term, introduced in Eq. (6), indeed corresponds to the additional optical path length ζ resulting from a beam axis displacement \bar{x} , \bar{y} . Let $dS \equiv (dz^2 + d\bar{x}^2 + d\bar{y}^2)^{1/2}$ be the elementary optical path length along the beam axis. The z derivative of ζ is

$$\begin{aligned} \dot{\zeta} &= N(\bar{x}, \bar{y}, z) dS/dz - N(0,0,z) \\ &\simeq (1 + n_x \bar{x} + n_{xx} \bar{x}^2 + n_y \bar{y} + n_{yy} \bar{y}^2 + n_{xy} \bar{x} \bar{y}) \left(1 + \frac{\dot{\bar{x}}^2}{2} + \frac{\dot{\bar{y}}^2}{2}\right) - 1 \\ &\simeq \frac{1}{2} \frac{d}{dz} (\bar{x} \dot{\bar{x}} + \bar{y} \dot{\bar{y}}) + \frac{1}{2} (n_x \bar{x} + n_y \bar{y}). \end{aligned} \quad (7)$$

The last expression of ζ , obtained with the help of Eqs. (5a) and (5b), readily gives the on-axis phase ζ by integration. For later convenience, the lower limits of integration 0_x and 0_y , in Eq. (6), are taken at the points where the rays \bar{x} and \bar{y} , respectively, intersect the z axis.

Equation (6) generalizes a result obtained by Tien and others¹¹ who have shown that the axis of a gaussian beam, injected slightly off-axis in an aligned lenslike medium, is a paraxial ray.[†] In the following sections, only the case of orthogonal media ($n_{xy} = 0$) is discussed.

III. Fundamental Gaussian Beams

An important solution of Eq. (4) is the fundamental gaussian beam, henceforth called, for brevity, gaussian beam. Let us give first the expression of the field of a gaussian beam injected along the axis of an aligned orthogonal medium ($n_x = n_y = n_{xy} = 0$):

$$\psi(x,y,z) = \left[X^{-1/2} \exp\left(-j \frac{k}{2} \frac{X}{X} x^2\right)\right] \left[Y^{-1/2} \exp\left(-j \frac{k}{2} \frac{Y}{Y} y^2\right)\right], \quad (8)$$

where X and Y are generally complex functions of z which satisfy Eqs. (5a) and (5b), respectively (with $n_x = n_y = n_{xy} = 0$). We call X and Y complex rays.[‡] When X and Y are real, Eq. (8) gives the field of a ray pencil limited to rays $X(z)$ and $Y(z)$ in the xz and yz planes, respectively. Its significance is then straightforward: the terms in front of the exponentials simply

* For clarity, only these real solutions are considered here. Complex solutions, however, are as well physically acceptable, even in the case where the losses are neglected.

† A result similar to Eq. (6) was obtained by H. E. Rowe (unpublished work, 1964) for the case of an aligned sequence of stigmatic lenses.

‡ Note added in proof: These complex rays result from paraxial approximation of rays originating from a point source whose position is complex. They are to be distinguished from the complex rays introduced by J. B. Keller [in *Calculus of Variations and its Application* (McGraw-Hill Book Co., New York, 1958)] for the calculation of the diffracted field in the shadow of a caustic.

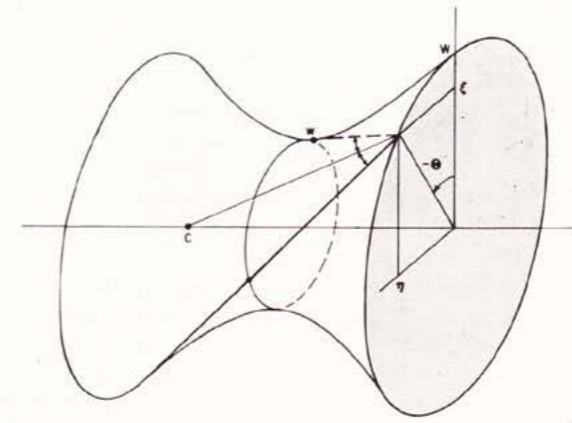


Fig. 1. This figure represents a fundamental gaussian beam as it propagates in free space. Its surface (hyperboloid of revolution) can be generated by a skew ray, represented by a plain line (or by its symmetric, represented by a dotted line), as it rotates about the axis. The bisectrix of the two skew rays intersects the axis at the wavefront center C .

result from the conservation of power since the ray pencil cross section area is proportional to XY . The arguments of the exponential terms are the phase shifts resulting from the wave surface curvatures.

Let us now show that a simple physical significance can also be attached to X (or Y) in the general case where it is complex. Equation (8) shows that the on-axis phase of ψ is*

$$\Theta \equiv \text{phase of } \psi(0,0,z) = -\frac{1}{2}[\text{phase of } X + \text{phase of } Y]. \quad (9)$$

Thus, for a rotationally symmetric beam ($X = Y$), the phase of X is equal to the on-axis phase, except for a minus sign. The on-axis phase shift θ experienced by a matched beam through an optical system whose ray matrix is $\begin{bmatrix} A & B \\ C & D \end{bmatrix}$ results from Eq. (9)†:

$$\theta = \cos^{-1}(A + D)/2; \quad (10)$$

θ is real when $|A + D| \leq 2$. It is taken in the $0-\pi$ interval.

Let us now express the beam radius W (defined as the distance from the axis where the field is reduced in intensity by a factor e) and the wavefront radius R , as

functions of \dot{X} and X . One obtains, from Eq. (8), setting $X \equiv \xi + j\eta$:

$$-j \frac{k}{2} \frac{\dot{X}}{X} x^2 \equiv -j \frac{k}{2} \frac{x^2}{R} - \left(\frac{x}{W}\right)^2, \quad (11a)$$

$$\frac{1}{W^2} = -\text{imaginary part of } \frac{k}{2} \frac{\dot{X}}{X} = -\frac{k}{2} \frac{\xi\dot{\eta} - \eta\dot{\xi}}{XX^*}, \quad (11b)$$

$$\frac{1}{R} = \text{real part of } \frac{\dot{X}}{X} = \frac{1}{2} \frac{d}{dz} \log(XX^*). \quad (11c)$$

It is henceforth assumed that n_{xx} and n_{yy} are real. In that case, both $\xi(z)$ and $\eta(z)$ obey the paraxial ray equation as well as $X(z)$. It is easy to verify, by differentiation with respect to z , and use of Eq. (5a), that the quantity $(\xi\dot{\eta} - \eta\dot{\xi})$, known as the Lagrange's invariant,¹⁰ is independent of z . This quantity can be set equal to $-2/k$, for convenience. Hence, from Eqs. (11b) and (11c), the modulus of X is equal to the beam width W , and the wavefront is perpendicular to the beam profile $W(z)$:

$$XX^* = W^2, \quad (12a)$$

$$R = W/\dot{W}. \quad (12b)$$

These results have important consequences, which are more easily seen if we represent $X(z)$ as a skew ray in a ξ, η, z rectangular coordinate system. This skew ray rotates about the z axis as the phase of X (i.e., the on-axis phase reference) is varied, and generates the beam surface, whose profile is $W(z)$. The beam profile is consequently the envelope of the rays $\xi(z)$, as shown before in slightly different forms.¹² Further, one observes that there are two symmetrical skew rays going through a given point on the beam surface. Because of the symmetry, the tangent to the beam profile at that point is the bisectrix of the skew rays. Since this property is preserved under projection, the bisectrix of any two projected skew rays intersects the axis at the wavefront center C (see Fig. 1), as shown by Steier.¹⁴ Figure 1 represents a gaussian beam as it propagates in free space. The skew rays are straight lines, in that case, and the beam surface is an hyperboloid of revolution. The representation of a gaussian beam by two rays, $\xi(z)$ and $\eta(z)$, provides a method of beam tracing which is more convenient, in some cases, than the Smith chart¹⁵ or lateral foci¹⁶ methods.

A gaussian beam is usually defined, at a given plane, by its radius W , its wavefront radius R , and its on-axis phase Θ . From Eqs. (9), (12a), and (11a), the complex ray X and its slope \dot{X} are related to these quantities by

$$X = W e^{-j\Theta}, \quad (13a)$$

$$\dot{X} = W e^{-j\Theta} [(1/R) - j(2/kW^2)], \quad (13b)$$

and we have

$$(X^* \dot{X} - X \dot{X}^*) = 4j/k. \quad (13c)$$

In free space, taking the origin of the z axis and the phase reference at the beam waist, of radius w , Eqs. (13a) and (13b) become:

$$X(z) = w - j(2/kw)z. \quad (14)$$

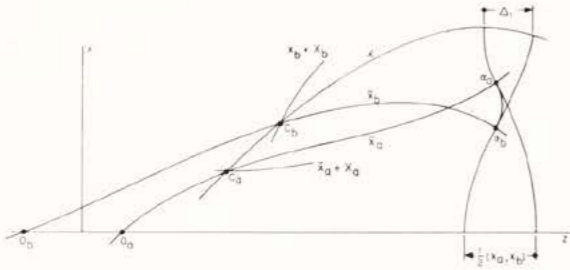


Fig. 2. \bar{x}_a and \bar{x}_b represent the axes of two ray pencils whose centers are C_a and C_b , respectively. χ is the ray which belongs to the two ray pencils. The five circles drawn in this figure for the construction of Δ_1 and $\frac{1}{2}(\bar{x}_a, \bar{x}_b)$ are normally intersecting the rays and the z axis; they can be considered as wave surfaces. The relation between the phase of the coupling factor and these quantities is outlined in the text.

In Sec. IV, the coupling between two gaussian beams of arbitrary orientation, whose fields are obtained upon substitution of Eq. (8) in Eq. (6), is calculated.

IV. Coupling Between Gaussian Beams

Let us consider two solutions Ψ_a and Ψ_b of Eq. (4), and define the coupling factor† between the two beams a and b by

$$c_{ab} = \iint_{-\infty}^{+\infty} \Psi_a \Psi_b^* dx dy. \quad (15)$$

c_{ab} does not depend on z as one easily verifies by differentiating c_{ab} with respect to z and substituting for $\dot{\Psi}_a, \dot{\Psi}_b$ expressions taken from Eq. (4), if we assume that $\Psi_a \dot{\Psi}_b^* - \Psi_b^* \dot{\Psi}_a$ decreases rapidly as x, y tend to infinity.

Let us now calculate the coupling factor between two gaussian beams, defined by their axes and complex rays: \bar{x}_a, X_a and \bar{x}_b, X_b , respectively, by introducing in Eq. (15) the expression of the fields obtained before [Eqs. (6) and (8)]. After integration and some rearrangements, one obtains the normalized coupling factor as the product of

$$c_{abz} = \left(\frac{j}{k}\right)^{\frac{1}{2}} (X_a X_b^*)^{-\frac{1}{2}} \exp \left[-j \frac{k}{2} \frac{(\bar{x}_a - \bar{x}_b, X_a)(\bar{x}_a - \bar{x}_b, X_b^*)}{(X_a X_b^*)} \right] \times \exp \left\{ j \frac{k}{2} \left[(\bar{x}_a, \bar{x}_b) - \int_{0_a}^z n_x \bar{x}_a dz + \int_{0_b}^z n_x \bar{x}_b dz \right] \right\} \quad (16)$$

by a similar expression relative to y . In Eq. (16), (α, β) stands for $(\alpha\beta - \beta\alpha)$. With the help of Eq. (5a), we

† We use the expression *coupling factor* rather than *complex coupling coefficient* as in Ref. (6), because the definition of the latter differs from Eq. (15) by a phase factor. The coupling factor is proportional to the intermediate frequency current generated in a large square law detector by two beams of nearly equal frequencies. This current is rigorously invariant, in a lossless medium, with respect to the detector position (H. Kogelnik, private communication).

may verify that all three terms in Eq. (16) are independent of the coordinate system. Notice, in particular, that both $\bar{x}_a - \bar{x}_b$ and X_a obey the paraxial ray equation with no n_x term, and that, consequently, $(\bar{x}_a - \bar{x}_b, X_a)$ is a Lagrange invariant.

The physical significance of the three terms in Eq. (16) of the coupling factor can be understood by evaluating directly the coupling factor between two ray pencils, defined by two (real) rays $\bar{x}_a, \bar{x}_a + X_a$ and $\bar{x}_b, \bar{x}_b + X_b$, respectively. The coupling between the pencil wave surfaces is significant only at the points where the phase of $E_a E_b^*$ is stationary, i.e., on the ray $\chi(z)$ which belongs to the two pencils; on that ray, the two wave surfaces, being normal to the same ray, are indeed tangent to each other. The intensity of the coupling is expected to be proportional to the field intensities, and to the area over which the two wave surfaces do not depart from each other by more than, say, a wavelength:

$$|c_{abz}| \propto X_a^{-\frac{1}{2}} X_b^{-\frac{1}{2}} \left(\frac{\dot{X}_a}{X_a} - \frac{\dot{X}_b}{X_b} \right)^{-\frac{1}{2}} = (X_a X_b)^{-\frac{1}{2}},$$

since \dot{X}_a/X_a and \dot{X}_b/X_b are the curvatures of the two pencil wave surfaces. The above expression is the first term in Eq. (16), to within a constant. From the same point of view, the phase of the coupling factor is expected to be related to the optical distance $\overline{C_a C_b}$ between the ray pencil centers C_a and C_b , shown in Fig. 2. Since the phases were defined at the points $0_a, 0_b$, where the rays \bar{x}_a, \bar{x}_b cross the z axis, the phase of the coupling factor must be equal to $-k\Delta_T$, with:

$$\Delta_T = \overline{C_a C_b} + \overline{C_b 0_b} + \overline{0_b 0_a} + \overline{0_a C_a},$$

where the upper bars indicate optical distances, taken along the rays or the z axis. Δ_T can be written as the sum of two terms:

$$\Delta_T = (\overline{C_a C_b} + \overline{C_b 0_b} + \overline{0_b 0_a}) + (\overline{0_a 0_a} + \overline{0_a 0_b} + \overline{0_b 0_a}) \equiv \Delta_1 + \Delta_2,$$

where α_a and α_b are any two points on \bar{x}_a and \bar{x}_b , respectively, which are intersected normally by a circle; this circle can be interpreted as a wave surface. The geometric construction of Fig. 2 shows that the first term Δ_1 is $\Delta_1 = \frac{1}{2}(\bar{x}_a - \chi, \bar{x}_b - \chi)$. The condition that, $\bar{x}_a, \bar{x}_a + X_a, \chi$ on one hand, and $\bar{x}_b, \bar{x}_b + X_b, \chi$ on the other hand, belong to the same ray pencils, can be written:

$$(\bar{x}_a - \chi, X_a) = (\bar{x}_b - \chi, X_b) = 0.$$

These relations show, after a few transformations, that $-jk\Delta_1$ is the argument of the first exponential term in Eq. (16).

The second term Δ_2 is, from Eq. (7),

$$\Delta_2 = \zeta_{\alpha_a} - \zeta_{\alpha_b} = \frac{1}{2} \left[\bar{x}_a \dot{\alpha}_a + \int_{0_a}^z n_x \bar{x}_a dz - \bar{x}_b \dot{\alpha}_b - \int_{0_b}^z n_x \bar{x}_b dz - (\bar{x}_a - \bar{x}_b)(\dot{\alpha}_a + \dot{\alpha}_b) \right] = -\frac{1}{2} \left[(\bar{x}_a, \bar{x}_b) - \int_{0_a}^z n_x \bar{x}_a dz + \int_{0_b}^z n_x \bar{x}_b dz \right].$$

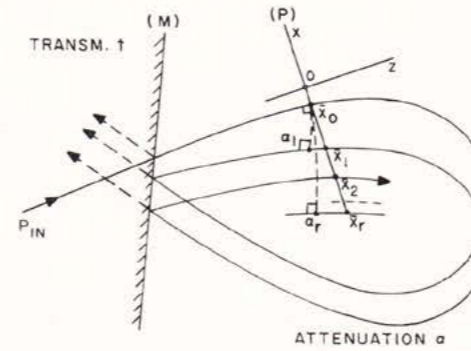


Fig. 3. This figure schematically represents a ring type cavity with an input-output mirror (M) of transmissivity t . (P) is an arbitrary reference plane in the ring path.

This expression shows that the argument of the second exponential term in Eq. (16) can be obtained by evaluating optical lengths along the beam axes.

V. Response of Arbitrary Optical Cavities

From the expression of the coupling factor between two gaussian beams derived in Sec. IV, the response of optical cavities excited by such beams can now be calculated.

Consider the ring type cavity shown schematically in Fig. 3, incorporating an input-output mirror (M) of transmissivity t , and let $\mathcal{L}^2 \equiv e^{-2\alpha}(1-t)$, where α is the field loss in the cavity, be the total power loss per round trip. The total power flowing through the reference plane (P) is, to within a constant,

$$P = \iint_{-\infty}^{+\infty} \sum_{r=0}^{\infty} E_r(x,y) \mathcal{L}^r \sum_{s=0}^{\infty} E_s^*(x,y) \mathcal{L}^s dx dy, \quad (17a)$$

$$P = \sum_{r=0}^{\infty} \sum_{s=0}^{\infty} \mathcal{L}^{r+s} c_{rs}, \quad (17b)$$

where $E_r(x,y) \mathcal{L}^r$ is the field of the input beam at (P) after r round trips, and the definition of Eq. (15) of the coupling factor has been used.

From the invariance property of the coupling factor, we have

$$c_{rs} = c_{0 \ s-r} \quad \text{if } r \leq s, \\ c_{rs} = c_{rs}^* = c_{0 \ s-r}^* \quad \text{if } r \geq s. \quad (18)$$

Let us call P_0 the value assumed by P in the absence of coupling between different paths ($c_{rs} = 0$ if $r \neq s$, $c_{rs} = 1$ if $r = s$) and define the cavity response by $T \equiv P/P_0$. From Eqs. (17) and (18), one obtains:

$$T = 1 + 2 \text{ real part of } \sum_{r=1}^{\infty} \mathcal{L}^r c_{or}. \quad (19)$$

Let us remark that, in first approximation, the frequency dependence of c_{or} is expressed by $\exp(jrkl_0)$, where l_0 is the cavity path length, and that, conse-

quently, the average response over a free spectral range [from $kl_0 = 2K\pi$ to $2(K+1)\pi$, K integer] is always unity, and does not depend on the excitation field.

Let us now calculate explicitly the coupling factors c_{or} for the case of a cavity defined by its round trip ray matrix. The input beam axis parameters $\bar{x}_0, \dot{\bar{x}}_0$ are transformed, after r round trips, into $\bar{x}_r, \dot{\bar{x}}_r$, given by the linear relations:

$$\begin{bmatrix} \bar{x}_r \\ \dot{\bar{x}}_r \\ 1 \end{bmatrix} = \begin{bmatrix} A & B & \delta \\ C & D & \delta \\ 0 & 0 & 1 \end{bmatrix}^r \begin{bmatrix} \bar{x}_0 \\ \dot{\bar{x}}_0 \\ 1 \end{bmatrix}. \quad (20)$$

In general ($A + D \neq 2$), the δ, δ terms can be eliminated by a proper choice of the coordinate system. This is not possible, however, when $A + D = 2$, if $\delta/\delta \neq (A-1)/C = B/(D-1)$. Because we are primarily interested in the latter case (misaligned degenerate cavities), the form Eq. (20) must be used. The complex ray X_0 defining the input gaussian beam, is transformed by:

$$\begin{bmatrix} X_r \\ \dot{X}_r \end{bmatrix} = \begin{bmatrix} A & B \\ C & D \end{bmatrix}^r \begin{bmatrix} X_0 \\ \dot{X}_0 \end{bmatrix}, \quad (21a)$$

$$\begin{bmatrix} X_r \\ \dot{X}_r \end{bmatrix} = \left\{ \cos r\theta \begin{bmatrix} 1 & 0 \\ 0 & 1 \end{bmatrix} + \frac{\sin r\theta}{\sin \theta} \begin{bmatrix} (A-D)/2 & B \\ C & -(A-D)/2 \end{bmatrix} \right\} \begin{bmatrix} X_0 \\ \dot{X}_0 \end{bmatrix}, \quad (21b)$$

since, as shown in Secs. II and III, X obeys the paraxial ray equation with no constant term. Equation (21b) has been obtained with the help of Sylvester's theorem.¹⁷

From the discussion of Sec. IV, the second exponential term in the expression of c_{or} is given by the total optical path length l_r between two points such as \bar{x}_0 and α_r , shown in Fig. 3, where a circle normally intersects the original beam axis $\bar{x}_0(z)$ and the r th beam axis $\bar{x}_r(z)$. Using the principle that two wave surfaces intercept equal optical lengths on the rays of a ray pencil, the following expression is obtained for l_r :

$$l_r = rl_1 + \frac{1}{2} \sum_{\rho=1}^r (\bar{x}_\rho - \bar{x}_0, \bar{x}_1 - \bar{x}_0). \quad (22)$$

It is important to notice that l_1 depends, in general, on the input beam axis position. Indeed, let us consider an input beam axis \bar{x}_0' different from \bar{x}_0 . Using the same method as above, the new path length is found to be

$$l_1' = l_1 - \frac{1}{2}(\bar{x}_0' - \bar{x}_1, \bar{x}_0 - \bar{x}_1'). \quad (23)$$

The second term on the right-hand side of Eq. (23) is not equal to zero, in general, and l_1' may differ from l_1 . Nevertheless, for a given input beam (defined by $\bar{x}_0, \dot{\bar{x}}_0, X_0$, and \dot{X}_0), a given cavity (defined by $A, B, C, D, \delta, \delta$, and \mathcal{L}) and a first-path length l_1 , Eqs. (19), (16), (20), (21b), and (22) completely define the response of the cavity to the incident beam. Let us write the expression of T for the case of beams with rotational symmetry ($Y_0 = X_0, Y_r = X_r$), and offsets lying in the xz meridional plane:

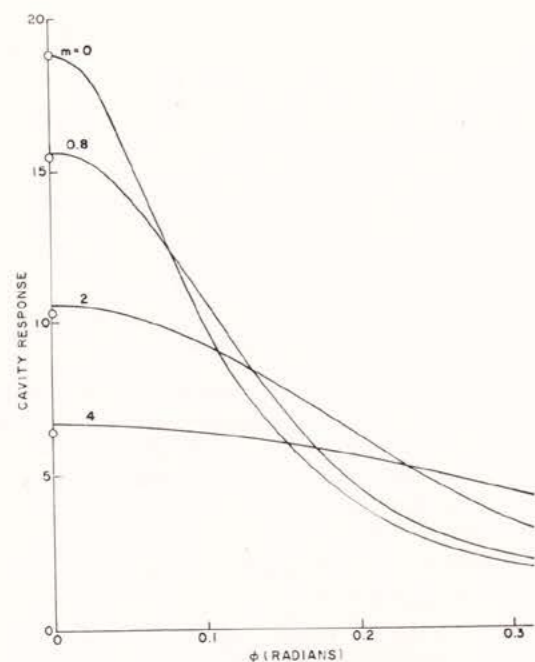


Fig. 4. Response of a degenerate cavity as a function of frequency for various degrees of misalignments, expressed by the parameter m ($m = 0$ to 4), for a round trip loss equal to 0.9 dB. The circles correspond to the small losses-small misalignment approximation.

$$T = 1 + 2 \text{ real part of } \sum_{r=1}^{\infty} \mathcal{L}^r \times \left(\frac{4j}{k} \right) (X_0, X_r^*)^{-1} \exp \left[-j \frac{k}{2} \frac{(\bar{x}_0 - \bar{x}_r, X_0)(\bar{x}_0 - \bar{x}_r, X_r^*)}{(X_0, X_r^*)} \right] \times \exp \left[-jkrl_1 - j \frac{k}{2} \sum_{\rho=1}^r (\bar{x}_\rho - \bar{x}_0, \bar{x}_1 - \bar{x}_0) \right], \quad (24)$$

where \bar{x}_r and X_r have to be replaced by their expressions, Eqs. (20) and (21b), respectively. The input beam radius W and phasefront curvature radius R , can be introduced in place of the complex ray parameters X_0 , X_0^* , with the help of Eqs. (13a) and (13b).

It is shown in Appendix that, in the case of conventional cavities, Eq. (24) is in exact agreement with results obtained from the Laguerre-Gauss or Hermite-Gauss mode theory. In Sec. VI, the case of misaligned mode-degenerate cavities is discussed.

VI. Response of Misaligned Mode-Degenerate Cavities

A cavity is *mode-degenerate* when its characteristic phase shift θ is equal to zero. All the latent roots of the 3×3 ray matrix [Eq. (20)] are then unity, and the r th power of this matrix can be evaluated from the confluent form of Sylvester's theorem (Ref. 17, p. 85):

$$\bar{x}_r = [1 + r(A - 1)]\bar{x}_0 + rB\dot{\bar{x}}_0 + \frac{r(r-1)}{2}(A\delta + B\dot{\delta}) + \frac{r(3-r)}{2}\delta, \quad (25a)$$

$$\dot{\bar{x}}_r = rC\bar{x}_0 + [1 - r(D - 1)]\dot{\bar{x}}_0 + \frac{r(r-1)}{2}(C\delta + D\dot{\delta}) + \frac{r(3-r)}{2}\dot{\delta}; \quad (25b)$$

X_r and \dot{X}_r are given by similar expressions without the constant terms:

$$X_r = [1 + r(A - 1)]X_0 + rB\dot{X}_0, \quad (26a)$$

$$\dot{X}_r = rCX_0 + [1 + r(D - 1)]\dot{X}_0. \quad (26b)$$

The case of strictly degenerate cavities ($A = D = 1$, $B = C = 0$) is of primary interest. Equations (25a), (25b), (26a), (26b), (22), and (23) become, respectively,

$$\bar{x}_r = \bar{x}_0 + r\delta, \quad (27a)$$

$$\dot{\bar{x}}_r = \dot{\bar{x}}_0 + r\dot{\delta}, \quad (27b)$$

$$X_r = X_0, \quad (27c)$$

$$\dot{X}_r = \dot{X}_0, \quad (27d)$$

$$l_r = rl_1, \quad (27e)$$

$$l_1' = l_1 + \frac{1}{2}(\bar{x}_0' - \bar{x}_0, \delta). \quad (27f)$$

Introducing Eqs. (27a)-(27e) in Eq. (24), the response of a misaligned degenerate cavity is found to be simply

$$T = 1 + 2 \sum_{r=1}^{\infty} \mathcal{L}^r \cos r\varphi \exp[-\frac{1}{2}r^2(k\Delta)^2], \quad (28)$$

where

$$\varphi \equiv kl_1, \quad \Delta^2 \equiv |(\delta_x, X)|^2 + |(\delta_y, Y)|^2. \quad (29)$$

For generality, the y parameters have been reintroduced in Eq. (29).

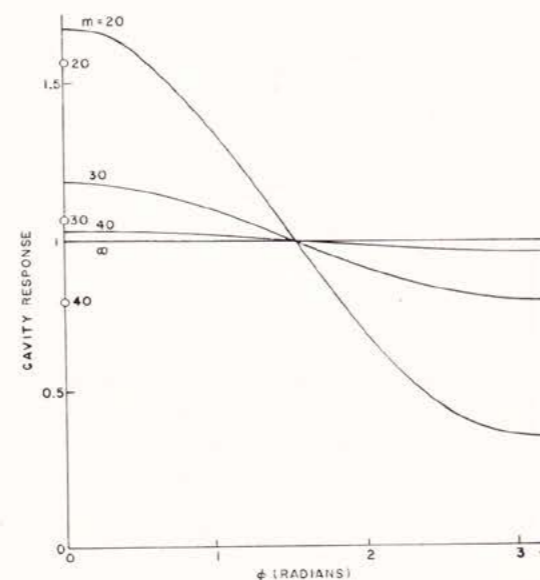


Fig. 5. This figure is a continuation of Fig. 4 for the case of large misalignments ($m = 20$ to ∞), with different scales. The circles correspond to the small losses-small misalignment approximation.

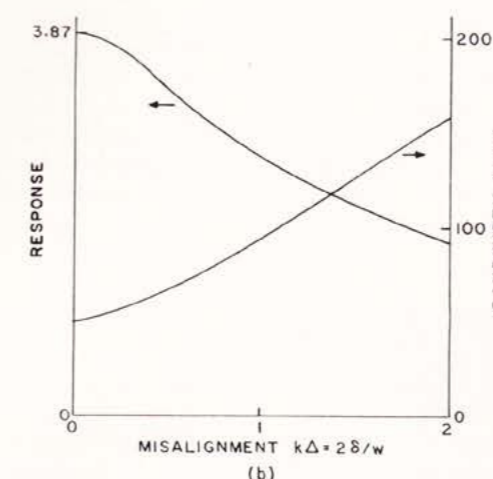
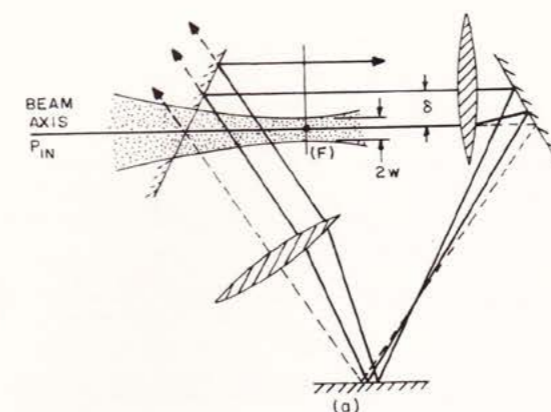


Fig. 6. A ring type cavity, degenerate in the ring plane, is represented in (a). Its theoretical response and bandwidth are shown in (b) as functions of the misalignment parameter $2\delta/w$, where δ is the lens offset and w the input beam waist radius, for a cavity round trip loss equal to 4.5 dB, and a round trip path length equal to 960 mm.

In the case of high cavity finesses and small misalignments, the sum in Eq. (28) can be replaced by an integral and T expressed in closed form with the help of error functions of complex arguments. Let us write down this expression at the resonance frequency ($\varphi = 0$):

$$T_{\varphi=0} = \frac{1 + \mathcal{L}}{1 - \mathcal{L}} \pi^{1/2} \left(\frac{1}{m} \right) \exp \left(\frac{1}{m^2} \right) \text{erfc} \left(\frac{1}{m} \right), \quad (30)$$

where

$$m \equiv k\Delta\mathcal{F}_0/(2^{1/2}\pi), \quad (31)$$

and $\mathcal{F}_0 = \pi/(1 - \mathcal{L})$ is the aligned cavity finesse.

T , as given by Eq. (28), is plotted as a function of φ , with the help of a computer, for $\mathcal{L} = 0.9$, and various values of m (Figs. 4 and 5). Figure 4 shows that the response of the cavity is reduced by 0.8 dB when the misalignment factor m is equal to 0.8 . Figure 5 is a

continuation of Fig. 4 with a different scale, and corresponds to the case of large misalignments. It shows how closely beams can be packed without introducing any substantial interference. The frequency dependence of the transmitted power does not exceed $\pm 3\%$, when m is larger than 40 . The response at the resonance, given by Eq. (30), is shown as circles in Figs. 4 and 5. One sees that this expression gives the actual response with a fairly good approximation when m does not exceed 4 .

As an example, let us apply Eq. (28) to the ring type cavity described in a previous paper.¹⁸ This cavity, which is represented in Fig. 6(a), incorporates two identical confocal lenses, and is degenerate in the ring plane. The incident beam waist, of radius w , is situated at the lens focal plane (F). One readily sees that the beam offset at that plane, after a round trip, is equal to the first lens offset δ , if the other cavity elements stay aligned.

From Eq. (14), we have $|X| = 2/kw$, and, from Eq. (29), $k\Delta = 2\delta/w$. The response and bandwidth of this cavity, as obtained from Eq. (28), are plotted in Fig. 6(b), as a function of the misalignment δ , for the set of parameters given in Ref. 18 (in the absence of laser discharge): the cavity gain is $\mathcal{L}^2 = 0.35$ (see Fig. 4 of Ref. 18) or $\mathcal{L} = 0.59$. Figure 6(b) shows that a misalignment $2\delta/w = 1.77$ results in a 3 -dB reduction in maximum response. This theoretical result is in acceptable agreement with the observed offset (Ref. 18): $2\delta/w = 2 \times 0.2 \text{ mm}/0.26 \text{ mm} = 1.55$. It results, from Eq. (27f), that the resonance frequency depends, in general, on the incident beam axis position. If the axis is tilted by an angle ν about the focal point F , for instance, Eq. (27f) shows that the resonance frequency variation becomes equal to the free spectral range when $\nu = 2\lambda/\delta$. No resonance frequency change occurs, however, if the incident beam is only offset.

In most applications, the cavity finesse is much higher than in the previous example, and the required accuracy in lens and mirror alignment is much more stringent. It is comparable to the one required for plane parallel Fabry-Perot etalons (which correspond to the case where $A = D = 1$, $C = 0$, $B = 2d$, d being the mirror spacing, in the previous equations).

Linear cavities can be considered as special cases of the ring type cavities considered before. The displacement of a single internal element, such as a lens, introduces, however, two misalignment terms per round trip. In special circumstances, these two terms cancel out as, for instance, in the internal lens confocal arrangement proposed by Pole.¹⁹ The position of this lens is not critical. The alignment of the two concentric end mirrors, however, stays critical. Another special case worth mentioning is the confocal cavity used with offset rays. This cavity is, in effect, equivalent to four confocal mirrors mechanically associated by pairs; its alignment is not critical, as it is well known. In general, two parameters have to be adjusted to align linear degenerate cavities properly (for instance, the tilt about the x and y axes of one end mirror), and four parameters in the case of ring type degenerate cavities.

VII. Nonorthogonal Misalignments in Degenerate Cavities

So far, cavities which can be analyzed by considering the behavior of rays in two perpendicular meridional planes have been discussed. In most ring type cavities, however, there are misalignments which cannot be reduced to the ones considered above because they couple the x and y parameters. These are associated with a *torsion* of the cavity path. Misalignments, however, always preserve the relative distances between the rays of ray pencils, to the first order. Since the most general continuous plane transformation which satisfies this condition is a rotation, the transformation resulting from small misalignments is, in general, a small rotation. The position of the center and the angle of this rotation depend on the specific misalignments introduced, but not on the incident beams considered. Since the transformation is repeated over and over for the successive paths, the successive beam pattern centers are evenly spaced along a circle.* [In the special case of orthogonal misalignments, the rotation axis of the transformation is at infinity and the transformation reduces to a translation, as shown by Eq. (27a)]. Such misaligned degenerate cavities tend to filter that part of the incident field which has a rotational symmetry about the rotation axis, since only such field configurations are reproduced after a round trip (unless the rotation angle is precisely an integral fraction of 2π , in which case other field configurations can resonate).

VIII. Conclusion

A simple expression for the response of degenerate cavities suffering from orthogonal misalignments has been derived; it was found to be in agreement with previously reported experiments. This expression can be written in closed form when the aligned cavity finesse \mathcal{F}_0 is large, and the internal lens offset δ is small. It shows that the cavity response decreases by 3 dB when $\delta = 5.5w/\mathcal{F}_0$, where w is the beam waist radius. The sensitivity of degenerate cavities to misalignments of their optical elements is consequently very high, except in a few special cases. The case of nonorthogonal misalignments has been shown to exhibit interesting features for application to nonresonant multipath systems and resonant spatial filters.

The field of view of a degenerate cavity is limited by aberrations, by the transverse variations of the mirror reflectivities, and by those of the gain when an active

medium is inserted in the cavity. Gaussian variations of the mirror reflectivities, and of the gain, can also be handled analytically, by attaching complex values to n_{xx} and n_{yy} . The calculations, however, would be more intricate than the ones given in this paper because the coupling factor is not invariant in that case. The reduction in field of view resulting from geometrical optics aberrations will be discussed in a forthcoming paper.²⁰

The author expresses his thanks to D. C. Hogg for useful comments.

Appendix. Response of Stable Cavities

In this appendix we show that the general Eq. (24), given for the response of an arbitrary cavity (stable, unstable, or mode degenerate), is consistent, for the case of conventional stable cavities, with results obtained from the Laguerre-Gauss or Hermite-Gauss mode theory.

In the case of stable cavities (θ nonzero real) an optical axis, i.e., a ray which retraces its path after a round trip, can be defined. Let l_0 be its optical length, Eq. (22) becomes

$$l_r = r l_0 + (x_0, x_r)/2, \quad (\text{A-1})$$

in agreement with Eq. (16).

Taking the z axis as tangent to the optical axis at the reference plane, the transformation of x_r is the same as the transformation of X_r , Eq. (21b). Since both x_r and X_r are now periodic functions of $r\theta$, the term under the sum sign in the Eq. (19) of the cavity response is also a periodic function of $r\theta$ multiplied by $\mathcal{L}^p e^{jr\varphi}$, where $\varphi \equiv k l_0$. In the limit where $\mathcal{L} \rightarrow 1$ (high cavity finesse), the cavity response consists of sharp peaks located at integral values of φ/θ , since, for these values of φ , the term under the sum sign becomes a periodic function of $r\theta$. Physically, these peaks correspond to the excitation of Laguerre-Gauss or Hermite-Gauss transverse modes.

Let us compare the intensity of these modes with the values obtained by Kogelnik⁶ on the basis of the Laguerre-Gauss mode theory, for the case of rotationally symmetric and coaxial cavities and beams. After some rearrangements, using Eq. (12a), the coupling factor can be written:

$$c_{or} = (\cos r\theta + jQ \sin r\theta)^{-1} e^{jr\varphi}, \quad (\text{A-2})$$

where Q is a mismatch factor[†]

$$Q = \frac{1}{2} \left[\left(\frac{W}{W_m} \right)^2 + \left(\frac{W_m}{W} \right)^2 \right] + \frac{k^2}{8} W^2 W_m^2 \left(\frac{1}{R} - \frac{1}{R_m} \right)^2. \quad (\text{A-3})$$

* If a radial offset is introduced with the help of a conical refracting plate, a spiraling spot pattern can also be generated. This is, however, a third-order geometrical optics effect, which is overlooked in the present discussion.

† With the notations of Ref. 6, $Q \equiv (2/\kappa) - 1$.

W and R are, respectively, the input beam radius and wavefront radius. W_m and R_m are the corresponding quantities for a matched beam. They are given, from the self-consistency equation¹² (except when $B = 0$), by

$$\frac{1}{R_m} - j \frac{2}{k W_m^2} = \frac{D - A}{2B} - j \frac{\sin \theta}{B}. \quad (\text{A-4})$$

When the input beam is matched to the cavity ($Q = 1$), c_{or} is equal to $\exp[jr(\varphi - \theta)]$, since the two beams are identical except for a phase shift $r(\varphi - \theta)$ experienced by one of them. Inserting Eq. (A-2) in Eq. (19), the response becomes

$$T = 1 + 2 \text{ real part of } \sum_{r=1}^{\infty} \mathcal{L}^r \frac{e^{jr\varphi}}{\cos r\theta + jQ \sin r\theta}. \quad (\text{A-5})$$

In the limit where $\mathcal{L} \rightarrow 1$ (high cavity finesse), and for $\varphi = \theta(1 + 2p) \pmod{2\pi}$, p being a nonnegative integer, the sum in Eq. (A-5) can be replaced by an integral over the interval $r\theta = 0$ to 2π . Taking $e^{jr\theta}$ as a complex variable, this integral is easily evaluated with the calculus of residues. Eq. (A-5) becomes

$$T_{\mathcal{L} \rightarrow 1} = \frac{1 + \mathcal{L}}{1 - \mathcal{L}} \frac{2}{Q + 1} \left(\frac{Q - 1}{Q + 1} \right)^p, \quad (\text{A-6})$$

in exact agreement with the result obtained from the Laguerre-Gauss mode theory.⁶ The integer p is now identified with the radial mode number of the field excited in the cavity. Equation (A-6) gives the power in transverse modes associated with a particular axial mode. Notice that the sum of $T(p)$ from $p = 0$ to ∞ does not depend on Q , as one expects from a previous remark. Numerical calculations show that the difference between the exact Eq. (A-5) and the approximation Eq. (A-6) of T does not exceed a few percent when $\theta = 0.65$, $Q = 1$ to 5 , and $\mathcal{L} \geq 0.9$, for $p = 0, 1, 2, 3$.

As another example, let us consider the case where the incident beam is matched to the cavity except for an offset \tilde{x}_0 and a tilt $\tilde{\alpha}_0$ of its axis. Let us substitute in Eq. (24) $X_0 e^{-jr\theta}$ for X_r , and assume, for simplicity, that $A = D$. In that case, we have $C/\sin \theta = -\sin \theta/B = -2/kw^2$, where w is the input beam radius. The coupling factor becomes

$$\begin{aligned} c_{or} &= \exp(-jr\theta) \exp[-(1 - \cos r\theta)|a|^2] \exp(jr\varphi - j \sin r\theta |a|^2) \\ &= \exp(-|a|^2) \exp[|a|^2 \exp(-jr\theta)] \exp[jr(\varphi - \theta)], \end{aligned} \quad (\text{A-7})$$

where

$$|a|^2 = (x_0/w)^2 + (kw\tilde{\alpha}_0/2)^2. \quad (\text{A-8})$$

In the limit where $\mathcal{L} \rightarrow 1$, and for $\varphi = \theta(q + 1)$, q being a nonnegative integer, Eq. (A-7) presents only one essential singularity at the origin ($e^{jr\theta} = 0$). The cavity response becomes

$$T_{\mathcal{L} \rightarrow 1} = \frac{1 + \mathcal{L}}{1 - \mathcal{L}} \frac{|a|^{2q}}{q!} \exp(-|a|^2). \quad (\text{A-9})$$

in exact agreement with the Hermite-Gauss mode theory [Ref. 7, Eq. (9)].

References

1. J. A. Arnaud, Appl. Opt. **8**, 189 (1969).
2. D. R. Herriott and H. J. Schulte, Appl. Opt. **4**, 883 (1965).
3. H. Kogelnik and T. J. Bridges, IEEE J. Quantum Electron. **QE-3**, 95 (1967).
4. A. G. Fox and T. Li, IEEE J. Quantum Electron. **QE-4**, 460 (1968).
5. H. Kogelnik, Appl. Opt. **4**, 1562 (1965).
6. H. Kogelnik, in *Proceedings of the Symposium on Quasi-Optics*, J. Fox, Ed. (Polytechnic Press, Brooklyn, 1964).
7. D. Gloge, Arch. Elek. Uebert. **20**, 82 (1966).
8. J. T. Verdeyen and J. B. Gerards, Appl. Opt. **7**, 1467 (1968). The expression of the coupling coefficient derived in Appendix A of this paper can also be found, in a more general form, in Ref. 7.
9. J. A. Arnaud and H. Kogelnik, Appl. Opt. **8**, 1687 (1969).
10. R. K. Luneburg, *Mathematical Theory of Optics* (University of California Press, Los Angeles, 1964).
11. P. K. Tien, J. P. Gordon, and J. R. Whinnery, Proc. I.E.E.E. **53**, 129 (1965); E. A. J. Marcetili, Bell Syst. Tech. J. **46**, 1733 (1967).
12. H. Kogelnik and T. Li, Appl. Opt. **5**, 1550 (1966).
13. V. P. Bykov and L. A. Vainshtein, Zh. Eksperim. Teor. Fiz. **47**, 508 (1964); W. K. Kahn, Appl. Opt. **4**, 758 (1965).
14. W. H. Steier, Appl. Opt. **5**, 1229 (1966).
15. S. A. Collins, Appl. Opt. **3**, 1263 (1964); T. Li, Appl. Opt. **3**, 1315 (1964); J. P. Gordon, Bell Syst. Tech. J. **43**, 1826 (1964); T. S. Chu, Bell Syst. Tech. J. **45**, 287 (1966).
16. G. A. Deschamps and P. E. Mast, in *Proceedings of the Symposium on Quasi-Optics*, J. Fox, Ed. (Polytechnic Press, Brooklyn, 1964); P. Laues, Appl. Opt. **6**, 747 (1967).
17. R. A. Frazer, W. J. Duncan, and A. R. Collar, *Elementary Matrices* (Cambridge University Press, New York, 1957).
18. J. A. Arnaud, I.E.E.E. J. Quantum Electron. **QE-4**, 893 (1968).
19. R. V. Pole, J. Opt. Soc. Amer. **55**, 254 (1965); see also D. R. Herriott, J. Opt. Soc. Amer. **56**, 719 (1966).
20. J. A. Arnaud, Bell Telephone Labs.; private communication.